Particle Emission in Heavy-Ion Reactions*

DONALD V. REAMES†
Lawrence Radiation Laboratory, University of California, Berkeley, California
(Received 18 August 1964)

Light charged particles produced at 0 deg in the interaction of 167-MeV O^{16} ions with Al, Ni, Ag, and Au thick targets have been analyzed magnetically with nuclear-emulsion detectors. The spectra obtained are compared with extensive statistical-model calculations, which include both the effects of angular momentum and of multiple particle emission. The spectra from light targets are seen to be sensitive to the equilibrium shape of the compound nucleus, since rotational effects that depend on this shape are large for these nuclei. For O^{16} on Au the de-excitation of the compound nucleus is found to be dominated by neutron emission, and a comparison of the calculations with neutron spectra seems to show that the nucleus fissions with highest probability after about 5 ± 1 stages of neutron emission. Owing to the increased competition of neutron emission, charged-particle evaporation for the heavier elements decreases so much that the observed spectra are dominated by direct reaction products. These products, particularly the Li isotopes, are seen to arise from a breakup of the incident O^{16}, and the energetics of this process are considered.

I. INTRODUCTION

WHEN a 167-MeV O^{16} ion strikes a target nucleus many processes can take place. In a distant or grazing collision nucleons may be exchanged between target and projectile, or more generally these collisions initiate the breakup of the projectile whose fragments continue in the general direction of the beam or are captured by the target nucleus.[1,2] As the collision distance is decreased it becomes possible for the target and projectile to amalgamate into a compound system in which the identity of the constituents is lost as the energy is shared among the participating nucleons. These compound nuclei, formed by heavy ions, are unique in that they can be produced in states of high angular momentum but with relatively low excitation. In their subsequent de-excitation, the distributions in angle and energy of the emitted particles are modified by the rotation to an extent that depends upon the properties of the rotating nuclei themselves.

Much of our understanding of the properties of highly excited compound systems is based on the liquid-drop model. Within the framework of this model, one can calculate[3–8] the equilibrium shape of a compound system and an associated moment of inertia that influences the energetics of the decay processes. For a fissioning system it is also possible to calculate the nuclear shape at the point of scission, which influences the fragment angular distribution and the energy dependence of the fission cross section. Particle spectra, on the other hand, are predicted to depend only on the nuclear shape at equilibrium and, in principle, allow an investigation of this shape for nuclei throughout the periodic table.

The dynamics of the de-excitation of highly excited nuclei have been treated on the basis of statistical theory first suggested by Bohr[9] and later examined at length by Bethe.[10] Although the dependence of energy-level densities on angular momentum was analyzed in detail by Bethe, the effect of this dependence on the particle angular distributions and spectra was not considered until recently,[11,12] when high angular momentum states became experimentally accessible.

The expectation of gaining some insight into nuclear equilibrium shapes and into the mechanism and extent of direct reactions has led to the measurement[13] and calculation reported here of the particle spectra in the forward direction, where the effects both of angular momentum and of direct reaction are expected to be greatest and where data were previously unavailable.

II. EXPERIMENTAL PROCEDURE

A. Experimental Arrangement and Exposure

The experimental arrangement is shown in Fig. 1. The O^{16} beam from the Hilac at Lawrence Radiation Laboratory was focused through the collimation system onto the target, which formed the rear of a Faraday cup. This target was sufficiently thick to stop the beam but

* Work done under the auspices of the U. S. Atomic Energy Commission.
† Present address: National Aeronautics and Space Administration, Goddard Space Flight Center, Greenbelt, Maryland.
[1] Richard Kaufmann and Richard Wolfgang, paper A-4 in *Reactions Between Complex Nuclei* (John Wiley & Sons, Inc., New York, 1960).
[2] Torbjørn Sikkeland, Eldon L. Haines, and Victor E. Viola, Jr., Phys. Rev. **125**, 1350 (1962).
[3] David Lawrence Hill and John Archibald Wheeler, Phys. Rev. **89**, 1102 (1953). References to earlier works on fission are found in this reference.
[4] I. Halpern and V. M. Strutinski, paper P/1513 in *Proceedings of the Second United Nations International Conference on the Peaceful Uses of Atomic Energy* (United Nations, Geneva, 1958), Vol. 15, p. 408.
[5] S. Cohen, F. Plasil, and W. J. Swiatecki, paper F-1 in *Proceedings of the Third Conference on Reactions Between Complex Nuclei* (University of California Press, Berkeley, 1963).
[6] G. A. Pik-Pichak, Zh. Eksperim. i. Teor. Fiz. **34**, 341 (1958) [English transl.: Soviet Phys.—JETP **7**, 238 (1958)].
[7] John R. Hiskes, Lawrence Radiation Laboratory Report UCRL-9275, 1960 (unpublished).
[8] Robert Beringer and W. J. Knox, Phys. Rev. **121**, 1195 (1961).
[9] N. Bohr, Nature **137**, 344 (1936).
[10] H. A. Bethe, Rev. Mod. Phys. **9**, 69 (1937).
[11] T. Ericson and V. Strutinski, Nucl. Phys. **8**, 248 (1958), and **9**, 689 (1958).
[12] Torleif Ericson, Advan. Phys. **9**, 424 (1960).
[13] Donald V. Reames, paper F-8 in *Proceedings of the Third Conference on Reactions Between Complex Nuclei* (University of California Press, Berkeley, 1963). (This paper is a preliminary report of earlier work on this experiment.)

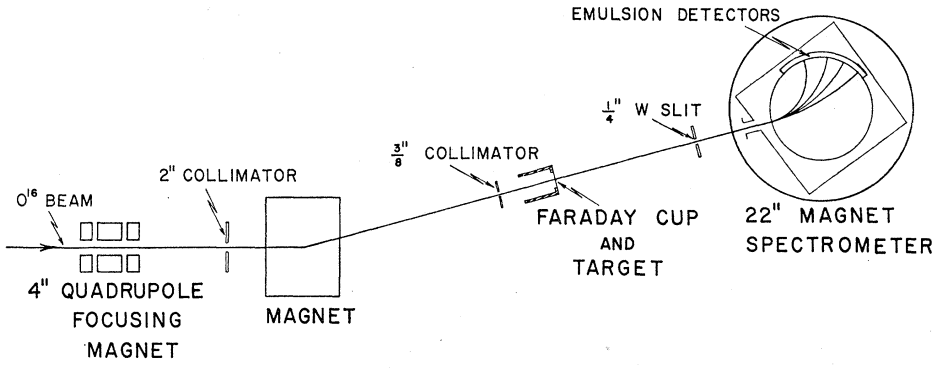

FIG. 1. Experimental arrangement.

allowed the lighter secondary particles to continue forward through a 0.25-in. slit into the spectrometer magnet, where they fell on the nuclear emulsion detectors placed around its periphery.

For the shorter range particles the emulsion used consisted of 1×3-in.×600-μ Ilford C.2 and K.5 glass-backed plates whose surfaces were inclined at 10 deg to the particle direction. Longer range particles were detected in small stacks, each composed of ten 1×3-in. ×600-μ pellicles, with the particles incident parallel to the surface through the 3-in. edge. Typical measurements of range versus deflection are shown in Fig. 2.

The target thicknesses were: Al, 71.19 mg/cm^2; Ni, 93.43; Ag, 108.53; and Au, 111.84 for bombardments with the 167-MeV beam (10.5±0.2 MeV/nucleon). Al was also bombarded at lower energy with a beam degraded to 142 MeV by an 11.62-mg/cm^2 Al foil placed in front of the quadrupole magnet (see Fig. 1) and falling on a 59.90-mg/cm^2 target. The two runs were made for Al to examine the beam-energy dependence of the yields, since this target allows reactions to occur over the largest range of energies, i.e., from 167 MeV to the Coulomb barrier at 30 MeV.

Collimators and slits used in this experiment were sufficiently thick to stop all but the very highest-energy particles observed, and their jaws were tapered a few degrees to minimize slit scattering. Contamination from the collimation system is calculated to be less than 1%.

B. Emulsion Scanning and Analysis

All energies measured in this experiment are based on ranges in the emulsion rather than on magnetic

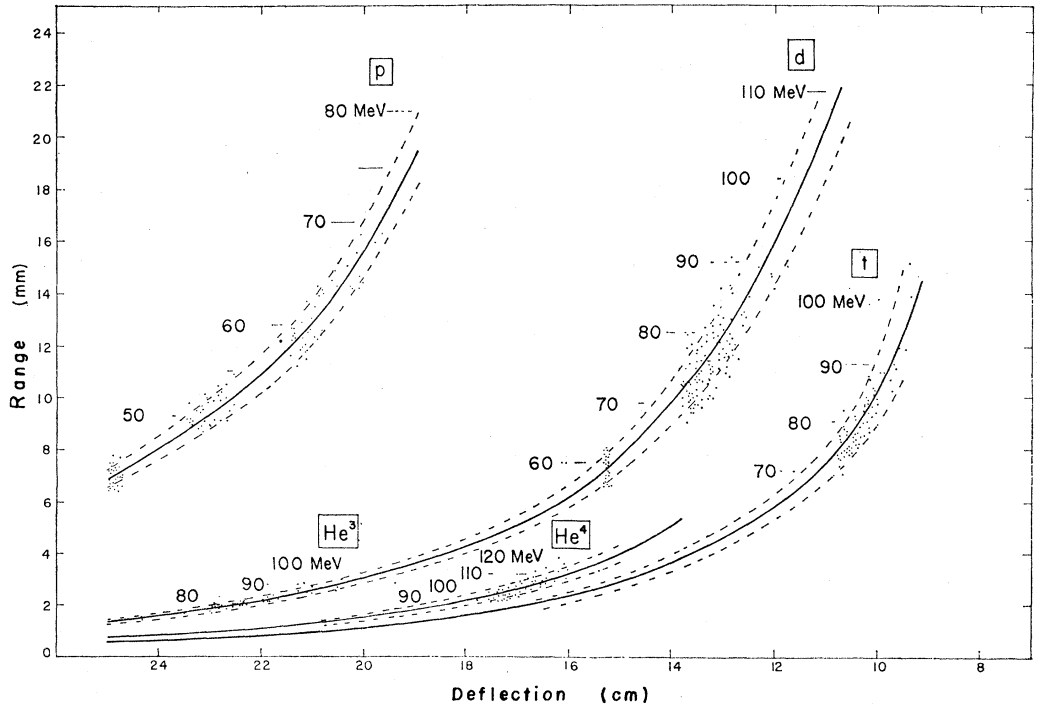

FIG. 2. Ranges of particles as a function of magnetic deflection for 167-MeV O^{16} on aluminum.

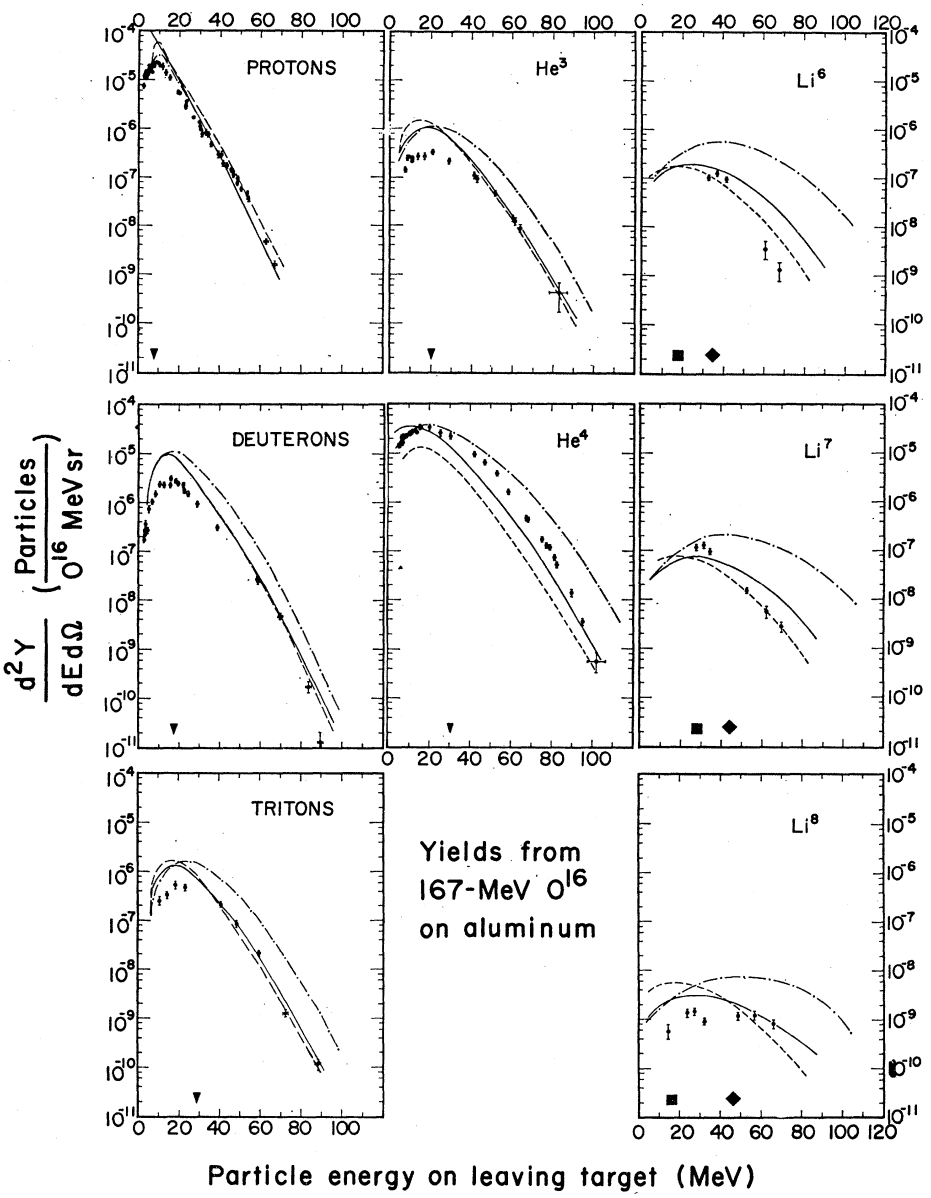

FIG. 3. Charged-particle yields at 0° from 167-MeV O^{16} on an aluminum thick target. Curves are the theoretical spectra, after the complete evaporation from the rotating nuclei, produced in spherical nuclei (dot-dashed curves), liquid drop shapes (solid curves), and with no rotation (dashed curves). Symbols at the bottom of the graphs indicate the energy at which direct products would appear under various assumptions (see text).

deflection. Where the particle densities were sufficiently great, however, the following simplifying procedure was adopted:

(a) At several points x_i on a plate the mean range (and hence $B\rho$) of a particular kind of particle was measured.

(b) The values at the different points were used to form a curve of $dB\rho/dx$ versus $B\rho$. This curve is universal for all particles and all targets, since it depends only on properties of the magnet, which were constant throughout the experiment.

(c) Measurement of the differential yield of a particle was therefore reduced to counting the number of particles N in an interval Δx, and measuring the mean range at the center of the interval. Thus if a particle kinetic energy T' is found from the range measurements, we have

$$\frac{\Delta^2 Y(T')}{\Delta\Omega\Delta T'}=\frac{1}{n_{ox}}\frac{N}{\Delta\Omega}\left(\frac{dT'}{dB\rho}\frac{dB\rho}{dx}\Delta x\right)^{-1}. \quad (1)$$

In this relation $dB\rho/dx$ is found from the curve described in step (b). The quantity n_{ox} is the number of oxygen ions collected on the Faraday cup, and the solid angle $\Delta\Omega$ is determined by the slit width and the vertical distance scanned.

In practice, of course, the experimental points themselves were used to determine the $dB\rho/dx$ points of step (b), which were then plotted versus $(B\rho)^2$ and fitted by a least-squares procedure to a straight line which is the

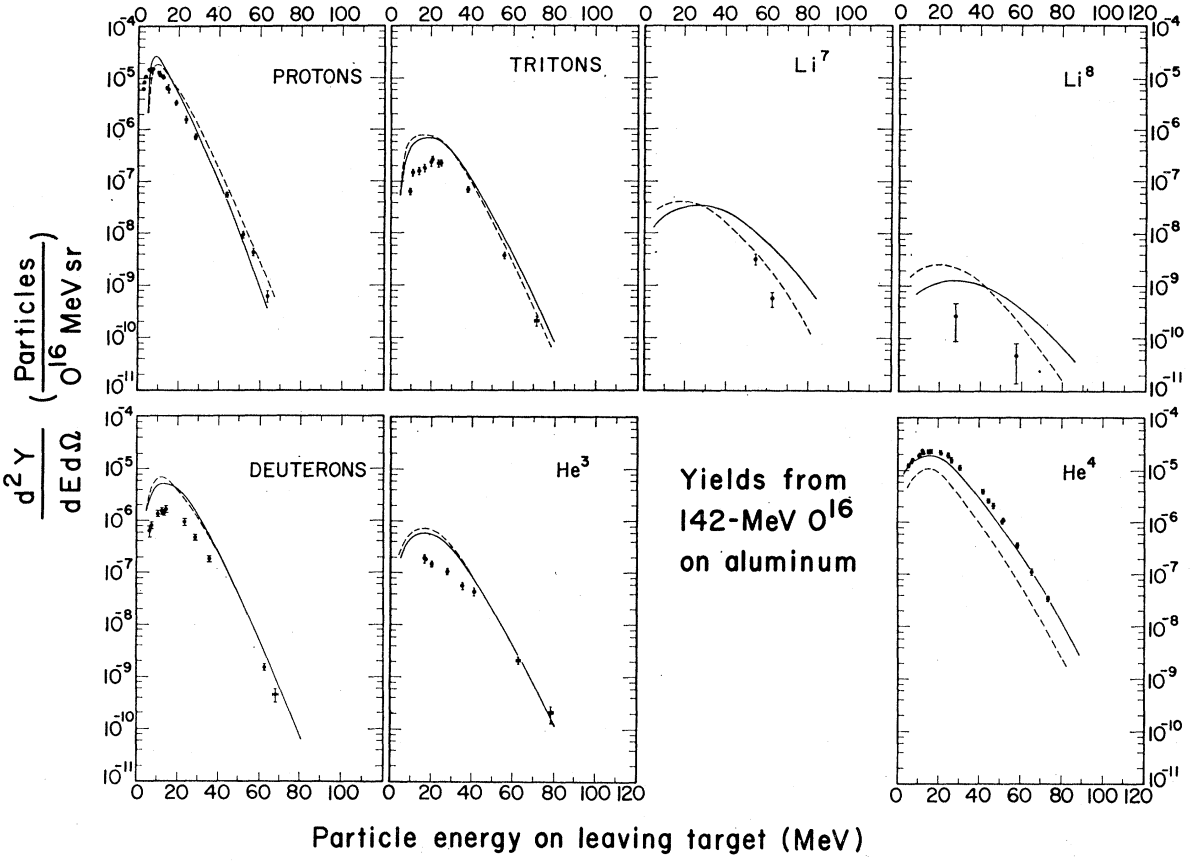

FIG. 4. Charged-particle yields at 0° from 142-MeV O^{16} on an aluminum thick target. Curves are the theoretical spectra, after the complete evaporation from the rotating nuclei, produced in the cases of liquid drop shapes (solid curves) and no rotation (dashed curves).

theoretical form for this function for a constant magnetic field. No systematic deviations from this form were detected, and the fitted curve probably gave at least as accurate a determination of the energy interval as would be given by other techniques.

When the number of particles varied rapidly with deflection, an entire region of the plate was scanned to find all particles in a given range interval, and the yield found was ascribed to the energy corresponding to the median range in the interval.

The emulsion range-energy relation used was taken from the work of Barkas.[14] These ranges differ by less than 1% in the region of interest from those given in a more recent work by the same author.[15] The ranges in standard emulsion were corrected (slightly) for the emulsion density of this experiment.

It is well known that certain particles, such as deuterons and He^3's have nearly the same range at a given magnetic deflection and hence are not resolvable by range measurements alone. This coincidence can occur only for particles of different charge, and in this experiment these particles could usually be distinguished visually by their track structure. The charge assignment was checked by standard emulsion techniques such as integral gap length measurement and δ-ray counting. Integral gap length measurements in C.2 emulsion distinguished deuterons and He^3's by more than two standard deviations in approximately 100μ of track length. Counting δ rays in K.5 emulsion gave an equal resolution with about 250μ of track.

Measurements were restricted to the spectra of isotopes of H, He, and Li, and no conclusions should be drawn about the production of a particle or isotope because it has not been included. Be isotopes were observed, for example, with cross sections comparable to those of Li. More highly charged products, in particular the easily identifiable B^8, would probably have been stopped by the target. The primary interest of this experiment was in the more common nuclear species, and further scanning for the more elusive particles could not be justified because of the difficulty involved in distinguishing them (or in observing them at all) in the experimental arrangement used here.

The experimental data are shown in Figs. 3 through 7. The error bars shown include errors in the energy

[14] Walter H. Barkas, Lawrence Radiation Laboratory Report UCRL-3769, 1957 (unpublished).
[15] Walter H. Barkas, *Nuclear Research Emulsions* (Academic Press Inc., New York, 1963), Vol. I, Chap. 10.

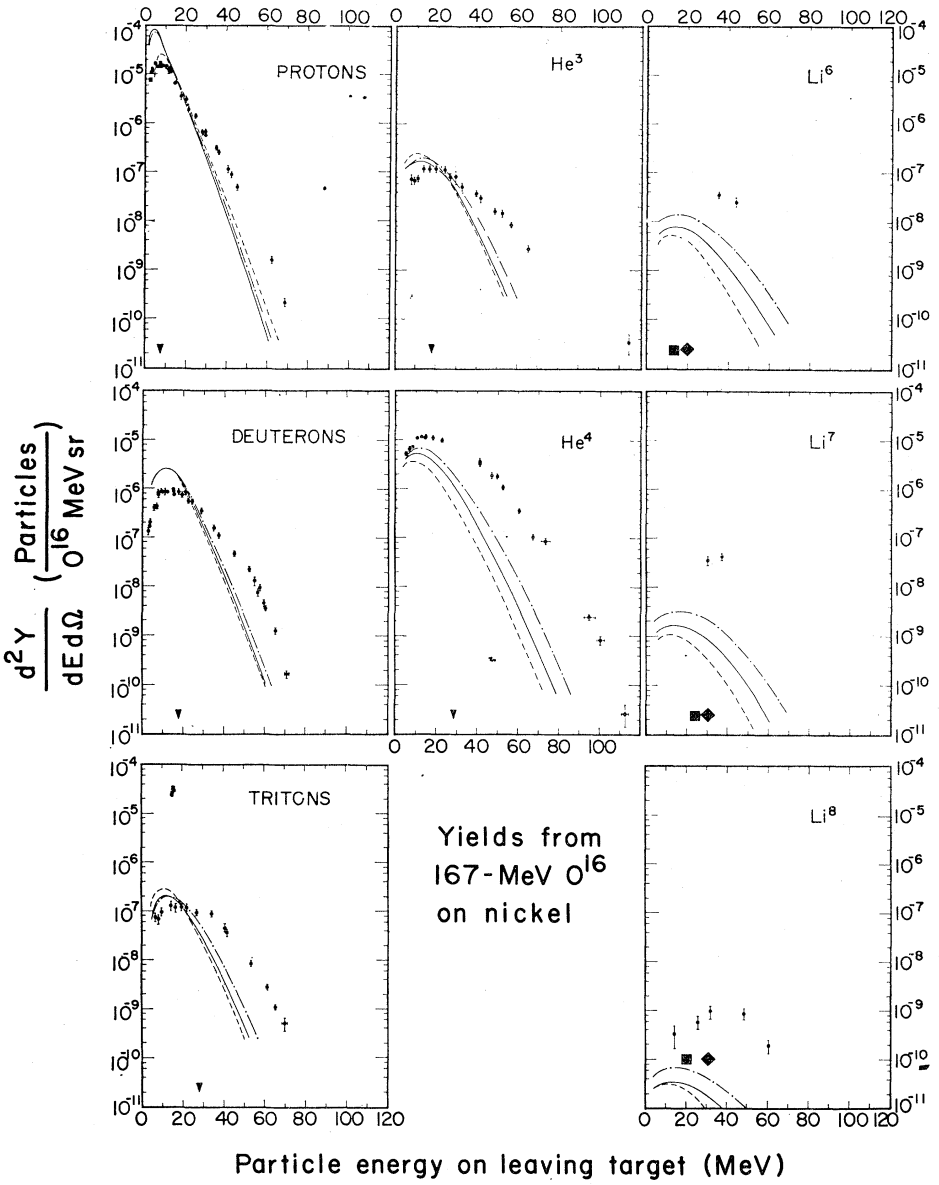

FIG. 5. Charged-particle yields at 0° from 167-MeV O^{16} on a nickel thick target. Curves are the theoretical spectra, after the complete evaporation from the rotating nuclei, produced in spherical nuclei (dot-dashed curves), liquid drop shapes (solid curves), and with no rotation (dashed curves). Symbols at the bottom of the graphs indicate the energy at which direct products would appear under various assumptions (see text).

measurements and experimental geometry as well as statistical errors. The particles under observation entered the surface or edge of a plate in a beam that was parallel to within a few degrees, and were easily distinguished from recoil protons produced by neutron scattering in the emulsion. Contamination of this type is expected to be completely negligible.

III. PARTICLE EVAPORATION

A. Statistical Theory

In order to develop the statistical theory of particle emission to be used here, we state the results of Ericson and Strutinski[11] and Ericson[12], which we then generalize to include multiple emission.

According to the principle of detailed balance, the probability per unit time P_{ab} for a transition from state a to state b is given by

$$P_{ab}\rho_a = P_{ba}{}^*\rho_b, \tag{2}$$

where ρ_a and ρ_b are the densities of states a and b. $P_{ba}{}^*$ denotes the probability of the time-reversed or inverse process.

We consider the state a to be an excited compound nucleus of spin **I**, and the state b to consist of both an emitted particle ν of kinetic (channel) energy $T_{c\nu}$ moving in a direction **n** and a residual nucleus R which has excitation energy U and spin **J**. We also make the classical approximation that the angular momenta **I** and **J** and the orbital angular momentum **l** are continuous

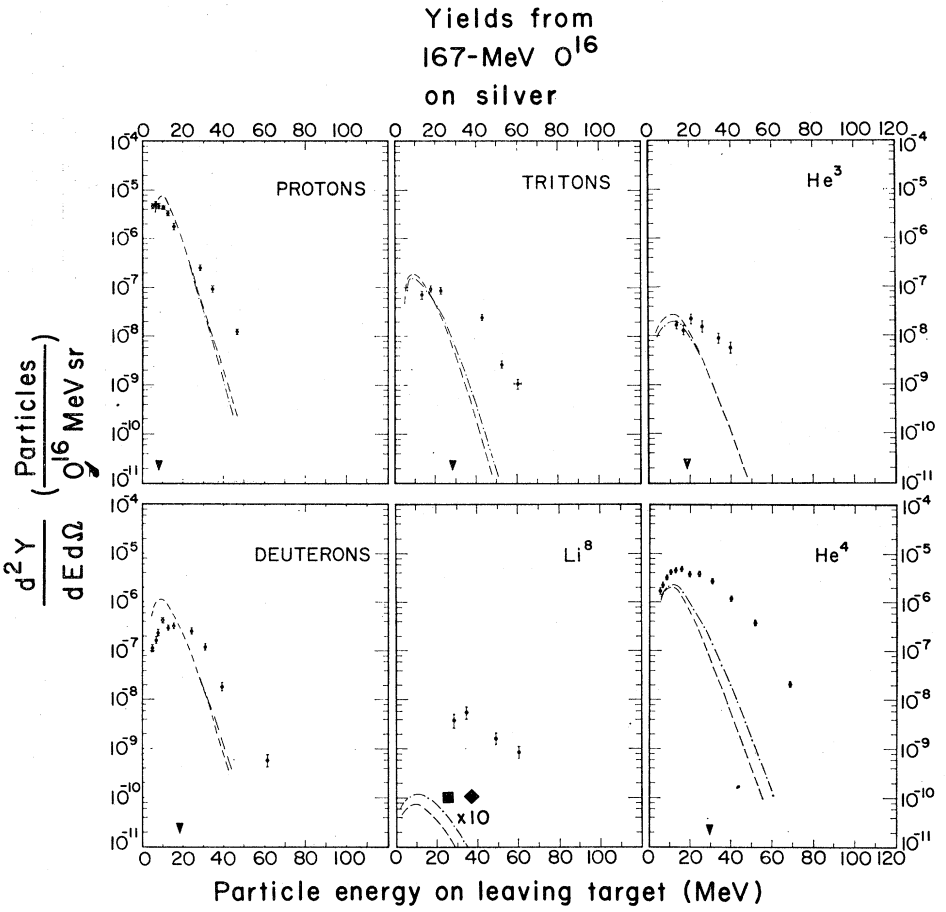

FIG. 6. Charged-particle yields at 0° from 167-MeV O^{16} on a silver thick target. Curves are the theoretical spectra, after the complete evaporation from the rotating nuclei, produced in spherical nuclei (dot-dashed curves) and with no rotation (dashed curves). Symbols at the bottom of the graphs indicate the energy at which direct products would appear under various assumptions (see text).

variables and that the direction of particle emission $\mathbf{n}$ is perpenducular to $\mathbf{l}$ (particle spin being considered only in the statistical weight factor $g_\nu=2s_\nu+1$ so that $\mathbf{I}=\mathbf{J}+\mathbf{l}$).

If $T_l(T_{c\nu})$ is the probability for the particle to penetrate the potential barrier of the nucleus with angular momentum $\mathbf{l}$, we may integrate over $\mathbf{J}$ and $\mathbf{l}$ and use Eq. (2) to write

$$\rho_c(\mathbf{I})P(T_{c\nu},\mathbf{n})dT_{c\nu}d\Omega_\nu = (d^3\mathbf{p}_\nu/h^3)g_\nu v_\nu\lambda^2\int\delta(\mathbf{n}\cdot\mathbf{l})T_l(T_{c\nu})d^3\mathbf{l} \times\int\delta^3(\mathbf{l}+\mathbf{J}-\mathbf{I})\rho_R(U,\mathbf{J})d^3\mathbf{J}. \quad (3)$$

The total probability of compound nuclear decay can be found by integrating $P(T_{c\nu},\mathbf{n})$ over $T_{c\nu}$ and Ω_ν, and we may therefore write the cross section for production of a particle ν as the product of the cross section for compound nucleus production times a normalized probability of decay, thus

$$\frac{d^2\sigma(T_{c\nu},\mathbf{n})}{d\Omega_\nu dT_{c\nu}} = \pi\lambda^2\int 2IT_I(E_c)\left[\frac{P(T_{c\nu},\mathbf{n})}{\sum_\nu\int\int P(T_{c\nu},\mathbf{n})dT_{c\nu}d\Omega_\nu}\right]dI, \quad (4)$$

where this result is presumed to have been averaged over ϕ_I.

B. Level Densities

The level density of rotating nuclei has been considered in some detail in the literature[10,12] and is treated only briefly here to illustrate the approximations made. A heuristic way to include the effect of rotation is to consider the rotational energy to be unavailable for excitation, so that

$$\rho(U,\mathbf{J})=\rho_0(U-U_R). \quad (5)$$

Thus if the level density for no rotation has the form

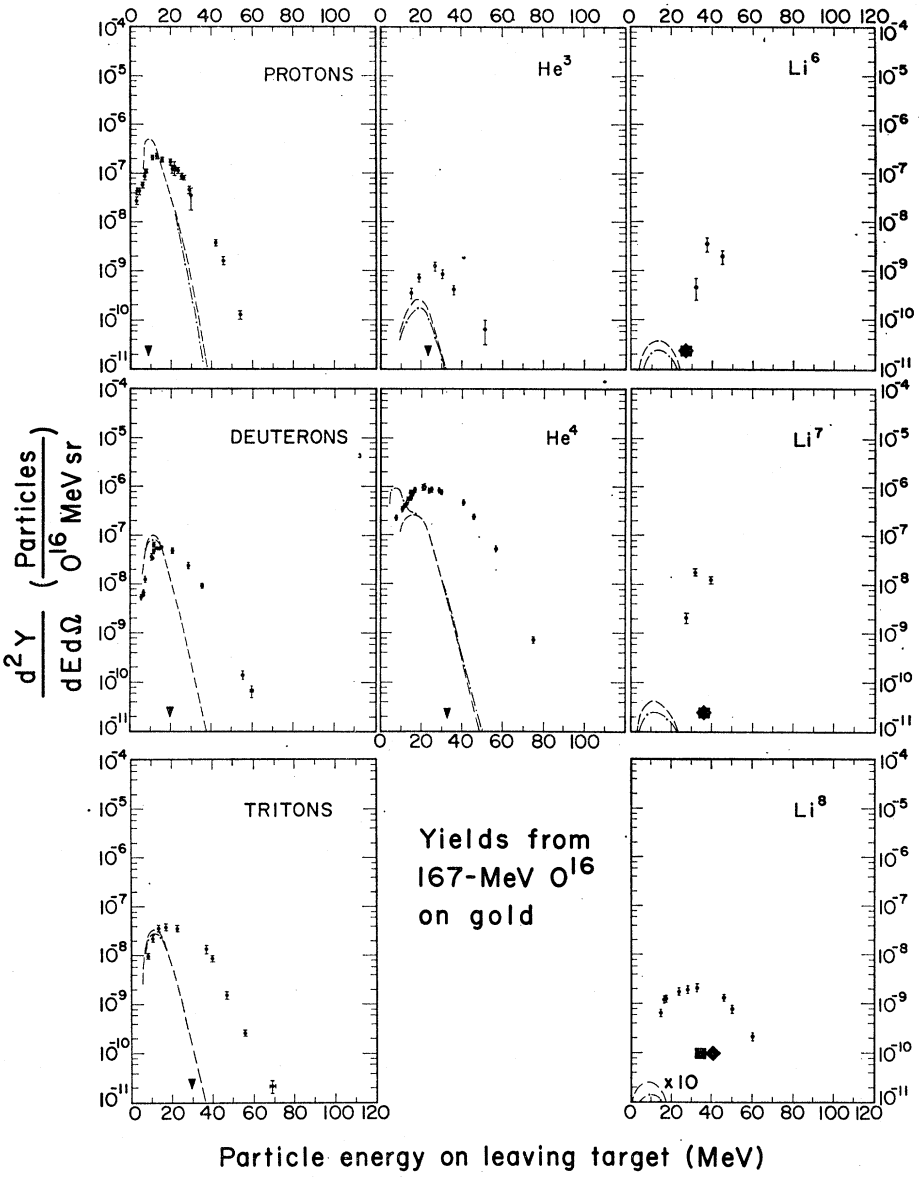

FIG. 7. Charged-particle yields at 0° from 167-MeV O^{16} on a gold thick target. Curves are the theoretical spectra, after the complete evaporation from the rotating nuclei, produced for spherical nuclei (dot-dashed curves) and with no rotation (dashed curves). Symbols at the bottom of the graphs indicate the energy at which direct products would appear under various assumptions (see text).

$\exp[2(\alpha U)^{1/2}]$, we now have

$$\rho(U,\mathbf{J}) \propto \exp\{2[\alpha(U-U_R)]^{1/2}\}, \quad (6)$$

which may be expanded for small U_R to give

$$\rho(U,\mathbf{J}) \propto \exp[2(\alpha U)^{1/2} - U_R/t], \quad (7)$$

where $t=(U/\alpha)^{1/2}$ is the nuclear (or, rigorously, the thermodynamic) temperature. The rotational energy may be written

$$U_R=\hbar^2 J^2/2\Im, \quad (8)$$

where $\Im$ is the nuclear moment of inertia.

Substituting (8) into the actual form of the level density used in the current calculations,[12] we have

$$\rho(U,\mathbf{J}) \propto (1/U^2 A_R^2)\exp[2(\alpha U)^{1/2} - \hbar^2 J^2/2\Im t], \quad (9)$$

where A_R is the atomic mass of the residual nucleus.

The level density parameter α has been shown[16,17] to have the approximate general form $\alpha=A_R/a$. For high excitation, deviations from this form due to shell effects are expected to disappear. In our calculations we have taken the temperature constant a to be 10 MeV unless otherwise noted.

Substituting (9) into (3), one finds that it is possible to do many of the integrations.[11] Combining the result

[16] D. W. Lang, Nucl. Phys. **26**, 434 (1961).
[17] David Bodansky, Ann. Rev. Nucl. Sci. **12**, 79 (1962).

with (4), we have the final form,[12]

$$\frac{d^2\sigma(T_{c\nu},\theta)}{d\Omega_\nu dT_{c\nu}}=\pi\lambda^2\int 2IT_I(E_c)dI\left\{\frac{g_\nu\int 2lT_l(T_{c\nu})(1/U^2A_R^2)\exp[2(A_RU/a)^{1/2}-(I^2+l^2)/2\sigma^2]W_{Il}(T_{c\nu},\theta)dl}{\sum_\nu g_\nu\int dT_{c\nu}\int 2lT_l(T_{c\nu})(1/U^2A_R^2)\exp[2(A_RU/a)^{1/2}-(I^2+l^2)/2\sigma^2]j_0(iIl/\sigma^2)dl}\right\}. \quad (10)$$

In (10),

$$1/\sigma^2=\hbar^2/2\Im t, \quad (11)$$

and

$$W_{Il}(T_{c\nu},\theta)=\frac{1}{4\pi}\sum_k(-1)^k(4k+1)\left[\frac{(2k)!}{(2^kk!)^2}\right]^2\times j_{2k}\left(\frac{iIl}{\sigma^2}\right)P_{2k}(\cos\theta). \quad (12)$$

Here j_n and P_n are the spherical Bessel function and Legendre polynomial of order n; θ is the angle between the directions of the emitted particle and the beam. We remark that our definition differs slightly from that of Refs. 11 and 12 in that W_{Il} is not normalized to 1, thus

$$\int W_{Il}(T_{c\nu},\theta)d\Omega_\nu=j_0(iIl/\sigma^2). \quad (13)$$

C. Multiple Emission

The excitation energy of the residual nucleus formed in the capture of a 167-MeV O^{16} ion can rarely be dissipated by the emission of a single particle and, in fact, the evaporation process may continue until as many as 8 or 10 particles are emitted. To account for this multiple emission in a rigorous way would be quite difficult. For each stage that contributes one would be forced to integrate over the energy spectra of all particles that could be emitted on each previous stage, the number of integrals increasing with the number of stages. For the large number of particles and stages to be considered here, this process obviously becomes prohibitive even without the inclusion of angular momentum.

An alternative procedure would be to use the particle-emission probabilities in Monte Carlo calculations. Such calculations have been made by Dostrovsky *et al.*[18] who ignored angular momentum. In such calculations, however, it is very difficult to determine the shape of the high-energy part of the spectra, since one must accumulate statistics in much the same way as in the experimental measurements themselves. Thus an accurate calculation of yields that vary over six orders of magnitude or of the yield of rare particles appears to be impractical.

Owing to the difficulties of these other methods, we have arrived at an average-value procedure for following the course of the evaporation. In this procedure the energy, mass, and charge removed by the particles are averaged over the energy spectrum of a particle and over the dominant particles. The results are then used to compute the properties of the residual nucleus which, in turn, emits more particles. Since the denominator in Eq. (10) is just such an integral over the particle spectrum and sum over the particles of the particle emission probability [see Eq. (4)], it may be treated as a weighting function (or operator), so that the mean value of a quantity X is

$$\bar{X}=\frac{\sum_\nu g_\nu\int dT_{c\nu}\int(X)2lT_l(T_{c\nu})(1/U^2A_R^2)\exp[2(A_RU/a)^{1/2}-(I^2+l^2)/2\sigma^2]j_0(iIl/\sigma^2)dl}{\sum_\nu g_\nu\int dT_{c\nu}\int 2lT_l(T_{c\nu})(1/U^2A_R^2)\exp[2(A_RU/a)^{1/2}-(I^2+l^2)/2\sigma^2]j_0(iIl/\sigma^2)dl}. \quad (14)$$

The spin of the residual nucleus and the associated coupling of **I** and **l** to form this spin were eliminated in the integration leading to Eq. (10). In order to compute the average spin of the residual nucleus (actually J^2 was averaged) we return to the level density in Eq. (9) and write

$$\langle\cos\theta_{Il}\rangle=\frac{\int_{-1}^{1}\cos\theta_{Il}\exp(Il\cos\theta_{Il}/\sigma^2)d\cos\theta_{Il}}{\int_{-1}^{1}\exp(Il\cos\theta_{Il}/\sigma^2)d\cos\theta_{Il}}, \quad (15)$$

which may be integrated explicitly. From this average we compute

$$\langle J^2\rangle=I^2+l^2-2Il\langle\cos\theta_{Il}\rangle, \quad (16)$$

which is then averaged as X in Eq. (14).

To find the contribution of a particular stage to the cross section, the properties of that stage are used to calculate the particle emission probability (expression in square brackets) in Eq. (10). The complete cross section is the sum over such stages.

[18] Israel Dostrovsky, Zeev Fraenkel, and Lester Winsberg, Phys. Rev. **118**, 781 (1960).

The evaporation procedure used here has the disadvantage that it does not correctly represent the increasingly wide spread of emitting nuclear species that occur on successive stages. It is possible, for example, to produce nuclei that in the last stage are constrained energetically to emit only one type of particle. This effect can produce an anomalously large contribution of these particles in the low-energy region of their spectrum. Examples of this behavior can be seen in Figs. 3 through 7. In truth, this final stage should be represented by many different species, some of which emit other particles. Also, as k increases, an increasingly large number of nuclei, emitting particles whose energy is higher than average, never reach the stage in question. In spite of these limitations many general features of this evaporation are faithfully reproduced and, as stated previously, it is perhaps the only practical technique available to us.

D. Moments of Inertia

If a nucleus could be treated as a spherical rigid body, its moment of inertia could be written

$$\Im_0=\tfrac{2}{5}(m_0A)(r_0A^{1/3})^2, \tag{17}$$

where m_0A is the mass, and $r_0A^{1/3}$ the radius of the nucleus. According to the liquid-drop model, the shape of the nucleus is distorted from sphericity because of its rotation and charge, so that the sum of the rotational, Coulomb, and surface energies is minimum.

When the rotational energy (referred to the surface energy of the sphere) is small the nucleus assumes an oblate spheriodal shape about the spin axis, as shown by Hiskes.[7] With increased rotational energy the nuclei undergo a transition to the prolate ellipsoidal shapes (rotating about an axis perpendicular to the symmetry axis) discussed by Beringer and Knox.[8] The change of these shapes with rotation has been studied throughout the periodic table by Cohen, Plasil, and Swiatecki,[5] and the moments of inertia based on these calculations[19] are used in this work.

These moments of inertia are tabulated as a function of the fissionability parameter $x=(Z^2/A)/50.13$ and rotational parameter, defined as $y=(\hbar^2J^2/2\Im_0)/17.81A^{2/3}$ for axes parallel and perpendicular to the symmetry axis. We have assumed that the particle emission is "sudden" in that the nucleus does not deform to adapt to its new spin **J** until after the particle is emitted. Under this assumption the symmetry axis to which the moments of inertia are referred lies parallel (for Hiskes shapes) or perpendicular (for Beringer-Knox shapes) to the initial spin **I**, but the moment of inertia about **J** depends on the angle between **J** and **I**, and hence on θ_{Il}. Conversely the angle θ_{Il} depends on the moment of inertia through Eq. (15), so that we have had to iterate Eq. (15) and the determination of $\Im$ to find the correct values of both $\cos\theta_{Il}$ and $\Im$. If the "sudden" assumption were incorrect we would be underestimating the moment of inertia.

A further dynamical assumption we have made is that a nucleus initially in a high-spin Beringer-Knox shape transforms into the low-spin Hiskes shape when the appropriate value of angular momentum is reached during the course of the evaporation.

Above a certain value of y, a nucleus is no longer stable.[5] This value of y was used to place a limit on the initial spin with which the compound nucleus could be formed.

Landau and Lifshitz[20] have shown that the only macroscopic motions possible for a gas in statistical equilibrium are uniform translation and rotation of the gas as a whole.[21] In the foregoing development we have therefore considered only rigid-body moments of inertia.[22] It is well known that for very low excitations, nuclear moments of inertia become smaller than those or rigid bodies,[23] but at such excitations one is dealing with more detailed properties of nuclear structure than are described by the statistical theory used here. One might expect that as the excitation energy is increased to the values of interest in this experiment, detailed properties—including shell and pairing structure—become lost and only the more gross properties remain. In the light of these considerations we have also neglected shell and pairing energies in calculating the masses of those highly excited nuclei, and have used the "reference" mass formula given by Cameron.[24]

E. Barrier Penetration

The escape of particles from the nucleus in the presence of Coulomb and centrifugal barriers is treated in any text on nuclear physics. The shape of the nuclear potential has been studied in electron scattering experiments[25] in terms of the Woods-Saxon[26] and Igo[27] potentials.

Hill and Wheeler have discussed penetration through inverted parabolic barriers and have related the penetration coefficient T_l to the height and curvature of the barrier.[3] We have used the potential

$$V_l(r)=zZe^2/r+l^2\hbar^2/2mr^2 \\ -50\exp[-(r-R)/0.574]. \tag{18}$$

[19] Franz Plasil (private communication).

[20] L. D. Landau and E. M. Lifshitz, *Statistical Physics* (Pergamon Press Ltd., London, 1958), see Sec. 10.

[21] The moment of inertia does depend on the shape of the potential used, as discussed by Claude Bloch, Phys. Rev. **93**, 1094 (1954).

[22] The use of rigid-body moments of inertia has been discussed by other authors; see, for example, Ref. 12, and J. R. Huizenga and R. Vandenbosch in *Nuclear Reactions*, edited by P. M. Endt and P. B. Smith (North-Holland Publishing Company, Inc., Amsterdam, 1962), Vol. II.

[23] Aage Bohr and Ben R. Mottelson, Kgl. Danske Videnskab. Selskab, Mat.-Fys. Medd. **27**, No. 16 (1954).

[24] A. G. W. Cameron, Can. J. Phys. **35**, 1021 (1957).

[25] Robert Hofstadter, Ann. Rev. Nucl. Sci. **7**, 231 (1957).

[26] Roger D. Woods and David S. Saxon, Phys. Rev. **95**, 557 (1954).

[27] George J. Igo, Phys. Rev. Letters **1**, 72 (1958).

In this expression m is the reduced mass of the emitted or incident particle and ze its charge. The radius R was taken to be

$$R=1.17\,A^{1/3}+r_1 \tag{19}$$

expressed in fermis, where A is the atomic weight of the target or residual nucleus and r_1 the radius of the incident or emitted particle. The particle radii (in fermis) used in the calculation of barrier penetration are: for n, 0; for p, 0; d, 2.11; t, 2.11; He^3, 1.61; He^4, 1.77; Li^6, 2.2; Li^7, 2.2; and Li^8, 2.2. These radii are based, in most cases, on the experimental values from Hofstadter,[25] and are felt to be slightly more realistic than the $1.17A^{1/3}$ form for these light particles. This latter form was used for the radius of the O^{16}.

By using the potential from (18) it is possible to calculate the barrier penetration coefficient[3]

$$T_l(E)=\{1+\exp[2\pi(B_l-E)/\hbar\omega_l]\}^{-1}, \tag{20}$$

where B_l is the height of the potential at its maximum and $\hbar\omega_l$ is related to the curvature at the same point by

$$\hbar\omega_l=|(\hbar^2/m)(d^2V_l/dr^2)|^{1/2}. \tag{21}$$

This procedure of replacing the true potential by an inverted parabola of the same height has been found to compare quite well with optical-model calculations.[28]

We should point out that this is the only part of our calculation in which the diffuseness of the nuclear potential has been taken into account. Other parts of the calculation are based on a square well with a radius parameter of 1.5 F. Attempts to include nuclear diffuseness in the level density for example, have been made by Beard,[29] but we have felt that the inclusion of such refinements was unjustified in this case. Barrier penetrability is perhaps more sensitive to the nuclear potential shape than are the other factors involved and, in fact, the inverted-parabola approximation is considerably simpler than an optical-model analysis with a square well.

F. Thick-Target Yield

In order to investigate the particle spectra at 0 deg we have stopped the O^{16} beam in the targets and measured the yields of particles rather than cross sections at a particular beam energy. To calculate such yields from the theoretical cross sections we first write the relation between the energy with which a particle leaves the target and the particle and beam energy at the point of interaction. By use of this relation, it is then possible to integrate over the beam energy and find the yield of particles at a particular observed energy.

Suppose an O^{16} ion of initial laboratory-system energy E_0 moves into the target and suffers a collision at a depth at which its energy has been reduced to the value E. From this reaction a particle of laboratory-system energy T_ν is emitted in the beam direction and is degraded in energy to the value T_ν' by the remaining thickness of target. The relation among the ranges that correspond to these energies can be written

$$R(T_\nu)-R(T_\nu')=D-[R(E_0)-R(E)], \tag{22}$$

where D is the target thickness.

We have previously shown[13] that the observed yield of particles may then be related to center-of-mass cross section for their production at the center-of-mass (channel) energy $T_{c\nu}$ by

$$\frac{d^2Y_\nu(T_\nu',0°)}{dT_\nu'd\Omega}=n_0\int_0^{E_0}\left[\left(\frac{T_\nu}{T_{c\nu}}\right)^{1/2}\frac{d^2\sigma(T_{c\nu},0°)}{dT_{c\nu}d\Omega_\nu}\right]\frac{dT_\nu}{dT_\nu'}\frac{dR(E)}{dE}dE, \tag{23}$$

where M_0 is the number of target atoms per cm,[3] and the differential cross section is calculated from (10) (summed over the evaporation). The quantity dT_ν/dT_ν' can be found from (22). All quantities in the integrand in (23) are considered to be expressed in terms of T_ν', and E by means of relation (22), and the relations between the channel and the laboratory-system energies at 0 deg. We have not considered the effect of the velocity of the recoil nucleus in the coordinate transformation for subsequent evaporation stages.

The range-energy relations for all charged particles in the different targets were taken from the work of Barkas and Berger[30] and were corrected for range extension owing to charge pickup, and for the effect of scattering on the range by the techniques described therein.

Most of the integrals in the calculations were computed by Gaussian quadratures, which are considerably more efficient than other standard methods but lend themselves less readily to analysis of calculational errors. In order to determine these errors typical calculations were compared with a Simpson's rule routine which increased the numbers of points calculated to achieve a desired accuracy.[31] From this comparison, the order of the Gaussian integration was chosen and a scheme was determined so that the limits of integration could be

[28] J. R. Huizenga and G. J. Igo, Argonne National Laboratory Report ANL-6373, 1961 (unpublished).

[29] David B. Beard and Alden McLellan, Phys. Rev. **131**, 2664 (1963).

[30] Walter H. Barkas and Martin J. Berger, Table of Energy Losses and Ranges of Heavy Charged Particle (to be included in National Academy of Sciences—National Research Council Publication 1133).

[31] As a comparison, the integrand for the integrations over l in Eq. (10) was calculated at an average of 10 points per integration, using the Gaussian integration. For equivalent accuracy a Simpson's-rule calculation required about 70 points. The particular Simpson's-rule routine used was quite fast and calculated additional points only in regions where the function contributed significantly to the integration (this routine was written by Leo Vardas of the Lawrence Radiation Laboratory, Livermore). With the Gaussian method the calculation took about 15 min per target per set of assumptions on the IBM-7094 computer.

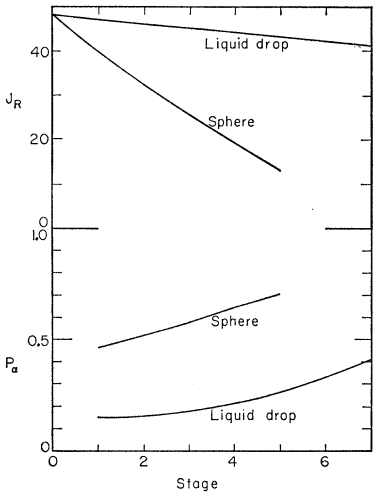

FIG. 8. Spin of the residual nucleus and probability of alpha-particle emission as a function of evaporation stage for evaporation from the compound nucleus produced with an initial spin of 48.2$\hbar$ by 167-MeV O^{16} on Al.

adjusted to encompass only the region of maximum contribution. Errors in the calculated cross sections due to the calculational methods alone, are never expected to exceed 10%, and are usually considerably less. The calculated yields could be in error by up to 15% where the yields themselves are small, but in most cases are well within a few percent.

G. Results of the Calculation

Before comparing the theoretical calculations with the data, we first discuss some facets of the calculations themselves. Figure 8 shows the spin of the residual nucleus and the alpha-emission probability as a function of the stage of evaporation for O^{16} on Al at the highest energy and angular momentum calculated. Since the liquid-drop moments of inertia used are larger, on the average, than that of a sphere, the rotational energy is smaller, and hence the effects of angular momentum are smaller. As a result the angular momentum is not removed as rapidly for this case, and the residual nucleus is left with an excessively large 41 units of angular momentum. The fact that we do not require the removal of this angular momentum (and thus do not really conserve energy) might have been anticipated when we expanded the level density exponent in (7). By using only the first term in this expansion, we underestimate the effect of rotation when U_R becomes comparable to U. If the correct density were used the integrations leading to (10) could not be done explicitly and the numerical calculations would have become prohibitive. We would expect intuitively that where the effects of rotation are large they should be *larger*, and where they are small they should become large on the latter stages of the evaporation. It should be noted that errors made near the end of the evaporation, such as those discussed here and in Sec. C, affect only the low-energy regions of the spectra of the dominant particles.

Referring again to Fig. 8, we see that the alpha-emission probability is considerably enhanced by the larger rotational energy. This occurs because the alphas are capable of removing more angular momentum for a given amount of energy than are the lighter particles. Still heavier particles are inhibited too strongly by the energetics. It can also be seen that the stronger rotational coupling effects a relative enhancement in the emission of higher-energy particles, which penetrate the angular-momentum barrier more easily. Since more energy is removed at a given stage, the nucleus evaporates for fewer stages.

The calculated yields are compared with the experimental results in Figs. 3 through 7. Calculations have been made with the liquid drop and spherical moments of inertia and for no rotation (infinite moment of inertia). For the heavier elements, for which rotational effects are small, the liquid drop calculations were omitted. The calculated and measured spectra are observed to disagree violently as one proceeds to increasingly heavier targets. Our analysis of the effects of angular momentum and of multiple emission shows that it is extremely unlikely that such phenomona could be responsible for the vast discrepancies between the observed and calculated spectra from these heavier nuclei. We are led to the conclusion, with Britt and Quinton,[32] that the production of charged particles from O^{16} bombardment of the heavier targets is dominated by noncompound-nuclear processes. Other features of the spectra, discussed below, support this conclusion. We would emphasize that this effect is relative in that it apparently owes its existence to a decrease in the evaporation of charged particles in favor of the evaporation of neutrons rather than an increase in the direct component itself with increasing target mass.

The higher energy products from oxygen on aluminum (Figs. 3 and 4) are seen to be fairly well described by the liquid-drop calculation. Though these calculations overestimate the yields of lithium isotopes, these are strongly influenced by the form of barrier penetration used, and the curves are almost an order of magnitude greater here than in our previous calculations,[13] for which classical barrier were used.

Calculations for the Ni target are compared with the results of this experiment in Fig. 5 and with the experiment of Knox, Quinton, and Anderson[33] in Figs. 9 and 10. It is immediately seen that the angular distributions of 16-MeV alphas in the backward hemisphere (Fig. 9) are not explained by the present calculations. Whether this is due to inadequacies of the assumptions used in the calculation, as mentioned previously, or to some mechanism in which all nucleons do not participate is not clear. The data do suggest an effect that is primarily rotational, owing to the approximate symmetry about 90 deg in the center of mass and the large forward and backward peaking.[33]

[32] Harold C. Britt and Arthur R. Quinton, Phys. Rev. **124**, 877 (1961).
[33] W. J. Knox, A. R. Quinton, and C. E. Anderson, Phys. Rev. **120**, 2120 (1960).

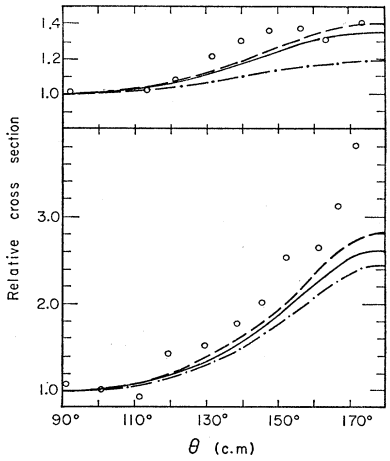

FIG. 9. Center-of-mass angular distributions of (upper) 10-MeV protons and (lower) 16-MeV alpha particles from 167-MeV O^{16} on Ni for spherical compound nuclei with temperature constants of 8 (dashed curves) and 10 MeV (solid curves) and for compound nuclei with shapes predicted from liquid drop theory with a=10 MeV (dot-dashed curves). Data are from Ref. 33.

In previous calculations based on an approximate expansion of the evaporation theory, it was suggested that nuclear moments of inertia might be considerably smaller than the relevant moment of inertia of a sphere, $\mathfrak{I}_0$.[33] Our treatment involves only more theoretically tenable moment of inertia which are, on the average, greater than $\mathfrak{I}_0$; yet we find anisotropies of the same magnitude as those calculated in Ref. 33. The increased coupling of **I** and **l** accounted for in our more rigorous treatment is the mechanism by which these anisotropies are achieved. In terms of the expansion, this coupling implies the alternative suggestion of Knox, Quinton, and Anderson, namely that $\langle l \rangle$ is increased rather than $\mathfrak{I}$ being decreased.

The alpha-particle spectrum at 90 deg in the center of mass (normalized by a factor of $\frac{2}{3}$) is compared with the data of Ref. 33 in Fig. 10. We see that a small shift in the peak energy still exists and we would not rule out a barrier lowering due to nuclear distortion suggested in that reference.

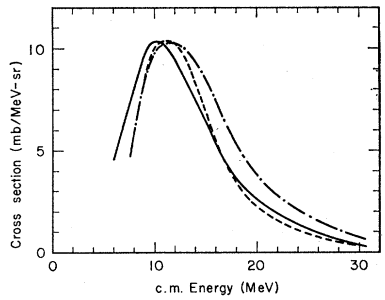

FIG. 10. Alpha-particle spectra at 90 deg in the center of mass from 167-MeV O^{16} on Ni. The solid curve is the data of Ref. 33 and is compared with the normalized theoretical spectra for liquid drop nuclei (dot-dashed curve) and spherical nuclei (dashed curve).

Though the charged particles emitted from oxygen on gold are controlled by direct mechanisms, we point out the calculated enhancement of low-energy alpha particles in the case in which rotation is included. This increase reflects an attempt of the nucleus to rid itself of its angular momentum in the later stages of evaporation by increased emission of alpha particles with respect to neutrons. Though this effect is of academic interest in alpha-particle emission, it is exactly this same effect which causes the nucleus to fission in preference to the emission of neutrons.

To investigate the competition between neutron emission and fission, we have compared Simon's neutron cross sections[34] with the evaporation calculations for spherical nuclei (the rotation has little effect on the neutron spectra here). In Fig. 11 these cross sections

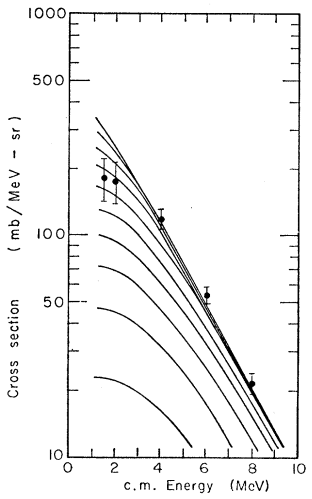

FIG. 11. Neutron cross sections at 90 deg in the center of mass from 167-MeV O^{16} on Au after each successive stage of evaporation. Data are from Ref. 34.

are presented after each stage has made its contribution to the evaporation at 90 deg in the center of mass. The calculated anisotropy is 1.08, and varies little with neutron energy and evaporation stage. This value is to be compared with the observed values listed in Table I. Simon argues that, contrary to the observations, the anisotropy of neutrons emitted from fission fragments would be expected to increase with neutron energy. The

TABLE I. Neutron spectrum at 90 deg c.m. and anisotropy (from Simon, Ref. 34).

Energy (MeV)	Cross section at 90° (mb/MeV-sr)	Anisotropy $\sigma(0°)/\sigma(90°)$
1.5	183±39	2.05±0.32
2.0	176±37	1.81±0.32
4.0	119±14	1.16±0.19
6.0	53.8±4.5	1.047±0.145
8.0	21.9±2.1	1.099±0.158

[34] William G. Simon, paper F-3 in *Proceedings of the Third Conference on Reactions Between Complex Nuclei* (University of California Press, Berkeley, 1963), and private communication.

higher energy neutrons (which are expected to be characteristic of the earlier stages of evaporation) agree in cross section and anisotropy with evaporation before fission.

Simon argues from the mean energy of the observed neutrons that the assumptions leading to an anisotropy of about 1.56 for 8-MeV postfission neutrons should be correct. If we assume that the compound nucleus evaporates three stages of 8-MeV neutrons at an anisotropy of 1.08, and that the rest of the observed cross section at this energy comes from postfission neutrons of anisotropy 1.56, we find that the observed anisotropy should be 1.29. A similar calculation for four stages of prefission neutrons gives an anisotropy of 1.22. This latter value is within one standard deviation of the observed value, so that we would expect *at least four* stages of neutron emission, on the average, before fission. Since the low-energy part of the spectrum has a greater anisotropy than expected (possibly because of the spin of the fragments) we have probably underestimated the postfission neutron anisotropy.

Though most of the low-energy postfission neutrons are not emitted at 90 deg, but are to be seen in the forward and backward directions, we would estimate conservatively from the lower energy portion of Fig. 11 and the associated anisotropies that *not more than six* neutrons, on the average, are evaporated before fission.

The calculated spectra for protons agree with the low-energy experimental values on about the fifth stage, and thus are consistent with the above arguments. We should further point our that any incorrect assumptions made about the angular momentum effects or multiple emission will probably not influence these results significantly, since the rotational energy is small and we are concerned only with the first few stages of emission.

The good agreement between the calculated and observed neutron spectra may be taken as further justification of our conclusions about the charged-particle spectra from heavy elements. The large discrepancy between theory and experiment in the latter case must, as stated previously, arise from the correctly predicted enhancement of neutrons relative to charged particles. As the target mass increases, charged-particle evaporation, as calculated, tends to become negligible with respect to the production of charged particles in direct processes.

IV. DIRECT PROCESSES

The large number of competing mechanisms that we categorize as primarily direct processes[35] makes any sort of quantitative analysis of their spectra very difficult. When single-nucleon transfer is known to occur or when the transferred nucleons may be treated as a single particle, analysis of the reaction has been successful.[36] It has been pointed out, however, that reactions that appear to be single-particle transfer can be strongly influenced by competing processes and by initial- and final-state interactions.[37]

Owing to this inherent complexity we have subjected the direct products observed here to an analysis based only on the energetics and the gross features of the spectra. In this spirit the triangle at the bottom of the graphs for hydrogen and helium isotopes indicates the energy at which these particles would appear if they were stripped from the oxygen at the same velocity it had as it entered the target at 167 MeV. None of these isotopes produced from the heavier targets is inconsistent with this interpretation.

The spectra of the hydrogen isotopes from O^{16} on Ni seem to show a statistically valid inflection in the region where they begin to depart from the calculated curve. This inflection suggests the presence of a competing mechanism which is either direct in nature or, at least, is a type of reaction characterized by a higher temperature (broader spectrum) suggesting that not all the nucleons participate.

Lithium isotopes have been treated on the basis of two assumptions. In either case they are presumed to be produced by the division of the full-energy O^{16} into a lithium and the equivalent of a boron nucleus, each of which gets a proportion of the available energy based on its mass. We then assume:

(a) The remaining boron is captured by the target nucleus.

(b) The boron exists as such, and is left free to continue into the target material.

The energy at which the lithium would appear under the first assumption is indicated by a diamond in Figs. 3, 5, 6, and 7; the lithium energy under the second assumption is indicated by a square.

A striking feature of the lithium spectra is that where the direct reactions are "resolved" (i.e., where the experimental yields far exceed the calculations or where double peaking phenomona are indicated) they occur with roughly equal yield independent of the target nucleus. This would indicate that they do indeed result from a breakup of the oxygen. Further, their production must depend strongly on beam energy, as can be seen by comparing the higher energy Li^8 production from the Al target at the two different beam energies. The low-energy portion of these spectra varies in proportion to the calculated evaporation curves.

Further theoretical and experimental investigation

[35] The term "direct process" is used here in the context of noncompound nucleus rather than in a more restrictive sense. Thus it covers any reaction mechanism in which the identity of the participants is not completely lost.

[36] See, for example, sessions B and C of *Proceedings of the Third Conference on Reactions Between Complex Nuclei* (University of California Press, Berkeley, 1963).

[37] I. S. Shapiro, Zh. Eksperim. i. Teor. Fiz. **41**, 1616 (1961) [English transl.: Soviet Phys.—JETP **14**, 1148 (1962)].

of these direct interaction processes would be of considerable interest, since one might hope to learn more of the details of the particle substructure of nuclei from them.

ACKNOWLEDGMENTS

The author wishes to express his thanks to Dr. Walter Barkas for his help and continued guidance throughout the course of this work, and to Dr. Harry H. Heckman and Dr. William G. Simon for numerous helpful discussions.

Thanks are also due the Visual Measurements group under Dr. Heckman, who did the emulsion scanning, C. Cole for his help in the emulsion processing, and Dr. Edward L. Hubbard and the crew of the Berkeley Hilac for their help in setting up and running the experiment.

The author also would like to thank Dr. Franz Plasil for making the results of his calculations available.

PHYSICAL REVIEW VOLUME 137, NUMBER 2B 25 JANUARY 1965

Further Evidence for the Nonexistence of Particle-Stable Tetraneutrons

S. CIERJACKS, G. MARKUS, W. MICHAELIS, AND W. PÖNITZ
Institut für Angewandte Kernphysik, Kernforschungszentrum Karlsruhe, Karlsruhe, Germany
(Received 9 September 1964)

A search was made for the occurrence of particle-stable tetraneutrons in the fast-deuteron-induced fission of uranium. This process is known to give a high yield of alphas and tritons. In order to deduce the presence of tetraneutrons, the following hypothetical reactions were investigated: $N^{14}(n^4,n)N^{17}$, $O^{16}(n^4,t)N^{17}$, $Mg^{26}(n^4,2n)Mg^{28}$, $Rh^{103}(n^4,2n)Rh^{105}$, $Bi^{209}(n^4,n)Bi^{212}$ and $Bi^{209}(n^4,2n)Bi^{211}$. No evidence for tetraneutrons was found. The upper limits of tetraneutron yields per alpha obtained from the above reactions are: 2×10^{-8}, 3×10^{-4}, 3×10^{-5}, 3×10^{-4}, 1×10^{-6}, and 1×10^{-8}, respectively. It seems reasonable to conclude from these results that the existence of tetraneutrons is most unlikely.

As a consequence of experimental results from the $He^4(\gamma,\pi^+)\rightarrow t+n$ reaction, it has been suggested that there is a low-lying resonant state in the n-t system at about 4 MeV above binding.[1] Since this state could not be observed in n-t scattering,[2] it has been interpreted as a state with isotopic spin[3] $T=2$. On the basis of this conclusion one would expect the existence of a particle-stable system of four neutrons bound by about[3] 4.5 MeV. However, reinterpretation of the experimental results shows that it is difficult to deduce from the hitherto existing data whether or not there is an H^4 state present in the reaction products.[4,5] In a recent experiment, an upper limit of 15% was obtained for the production of an H^4 final state.[6] The possible occurrence of He^8 and pairing energy arguments cast some doubt upon the stability of the tetraneutron, although the suggestion in favor of it cannot be rejected entirely.[7] Symmetry considerations allow the conclusion that the proposed $T=2$ resonance state implies the $T=1$ state of H^4 to be bound.[8] However, no H^4 was found in several searches.[9]

The problem of the states n^4 and H^4 is closely connected with the problem of the excited states of the He^4 nucleus and the existence of[7,10] H^5. A He^4 level at about[11,12] 20.1 MeV with[13] $T=0$ seems to be well established. In a recent paper a second excited state has been proposed at about[12] 21.2 MeV. It can be either a $T=0$ or a $T=1$ state. On account of isotopic spin conservation, all experiments up till now concerning the He^4 level structure cannot provide information on

[1] P. E. Argan, G. Bendiscioli, A. Piazzoli, V. Bisi, M. I. Ferrero, and G. Piragino, Phys. Rev. Letters **9**, 405 (1962).
[2] T. C. Griffith and E. A. Power, *Nuclear Forces and the Few Nucleon Problems* (Pergamon Press, London, 1960), Vol. I, pp. 473, 481, 511, and 517.
[3] P. E. Argan and A. Piazzoli, Phys. Letters **4**, 350 (1963).
[4] E. Lehrmann, H. Meyer, and H. O. Wüster, Phys. Letters **6**, 216 (1963).
[5] F. von Hippel and P. P. Divakaran, Phys. Rev. Letters **12**, 128 (1964) [see also erratum, Phys. Rev. Letters **12**, 497 (1964)].
[6] J. H. Smith, L. Criegee, G. Moscati, and B. M. K. Nefkens, Bull. Am. Phys. Soc. **9**, 420 (1964).
[7] V. I. Goldanskii, Phys. Letters **9**, 184 (1964).
[8] J. P. Schiffer and R. Vandenbosch, Phys. Letters **5**, 292 (1963) (see footnote).
[9] R. R. Carlson, E. Norbeck, and V. Hart, Bull. Am. Phys. Soc. **9**, 419 (1964). B. M. K. Nefkens and G. Moscati, Phys. Rev. **133**, B17 (1964). R. V. Popić, B. Z. Stepančić, and N. R. Aleksić, Phys. Letters **10**, 79 (1964). P. C. Rogers and R. H. Stokes, Phys. Letters **8**, 320 (1964) and references cited therein.
[10] V. I. Goldanskii, Zh. Eksperim. i Teor. Fiz. **38**, 1637 (1960) [English transl.: Soviet Phys.—JETP **11**, 1179 (1960)].
[11] P. G. Young and G. G. Ohlsen, Physics Letters **8**, 124 (1964) and references cited therein. S. Hayakawa, N. Horikawa, R. Kajikawa, K. Kikuchi, H. Kobayakawa, K. Matsuda, S. Nagata, and Y. Sumi, Phys. Letters **8**, 333 (1964).
[12] J. F. Mollenauer, Proceedings of the EANDC Conference on the Automatic Acquisition and Reduction of Nuclear Data, Karlsruhe, 1964 (unpublished), p. 205.
[13] C. Werntz, Phys. Rev. **128**, 1336 (1962). C. Werntz and J. C. Brennan, Phys. Letters **6**, 113 (1963). T. Stovall and M. Danos, Phys. Letters **7**, 278 (1963). H. Hackenbroich, Bull. Am. Phys. Soc. **9**, 505 (1964).